IJRCS

International Journal of Robotics and Control Systems
Vol. 3, No. 1, 2023, pp. 32-49
ISSN 2775-2658
http://pubs2.ascee.org/index.php/ijrcs

ASCEE

Multi-objective Fractional Order PID Controller Optimization for Kid's Rehabilitation Exoskeleton

Intissar Zaway [a,1,*], Rim Jallouli-Khlif [a,b,2], Boutheina Maalej [a,3], Hanène Medhaffar [a,4], Nabil Derbel [a,5]

[a] University of Sfax, ENIS, Laboratory of Control & Energy Management (CEM-Lab), Sfax, Tunisia
[b] Higher Institute of Computer Science and Multimedia of Sfax, Tunisia.
[1] intissarzaway18@gmail.com; [2] rim.jalloulikhlif@isims.usf.tn; [3] maalej.boutheina@gmail.com;
[4] hanene.medhaffar@isgis.usf.tn; [5] nabil.derbel@enis.tn
[*] Corresponding Author

ARTICLE INFO

Article History
Received November 13, 2022
Revised December 25, 2022
Accepted December 30, 2022

Keywords
Rehabilitation Robot;
Fractional order PID Controller;
PID Controller;
Optimization;
Genetic Algorithm;
Robustness

ABSTRACT

Fractional order Controllers have been used in several industrial cases to achieve better performance of the systems. This paper proposes a Fractional Order Proportional Integral Derivative (FOPID) controller. It is synthesized using Oustaloup approximation, and its parameters are tuned using the Genetic Algorithm (GA) optimization method. The aim is to minimize the error, the energy and the startup torques using two objective functions to improve the control performances and the robustness. The validity of the proposed controller is shown via simulation by controlling a two-link exoskeleton for children's gait rehabilitation, and the results are compared to an Integer order PID (IOPID) controller. Simulation results clearly indicate the superiority of the optimized FOPID in terms of trajectory tracking and the used torques. Moreover, the FOPID controller is tested with parameter uncertainties. Its robustness is proven against thigh and shank masses variation. Both controllers are simulated under the same frequency conditions using Simulink MATLAB R2018a.

1. Introduction

Cerebral Palsy (CP) is a nonprogressive neuromuscular motor disorder that affects the motor control of skeletal muscles and it is caused by a damage of the brain before, during, or shortly after the birth. Finding alternative treatments to improve the cognitive and motor skills of children with CP has a fundamental importance [1]. The goal of the rehabilitation is to improve the independence due to the progressive musculoskeletal pathology which occurs in most affected children in order to enhance the quality of the life for both patient and his family [2].

In recent years, a number of rehabilitation approaches has been reported for children with CP. In addition to conventional therapy which is done by a physiotherapist, robot systems might be beneficial for improving the gait ability and the lower limb skills. These novel technologies have been primarily developed for adults, then implemented in the pediatric field [3]. These systems allow the performance of an increased number of repetitions per session. Children with CP would benefit from periods of intensive physiotherapeutic interventions enhancing motor development, especially during intense growth periods and after surgical interventions. Moreover, the robotized rehabilitation provides the brain stimulation and accelerates the process of the therapy [4].

Several devices were designed for this purpose, like ReWalk [5], HAL[6], Ekso [7] and HANK [8]. All these devices help doctors and carry a suitable therapy goals. Focusing on these systems and like any other automatic devices, their mechanical architecture is under command. This is provided by the controller. At present, there is no general convergence in the control strategies of the exoskeleton, which is mainly due to the vast diversity in the design purposes, hardware structures, and actuating modes of different exoskeletons [9]. It can be fuzzy [10], neural network [11], adaptive [12], sliding mode [13] or PID controller [14].

The feedback compensator structure (the Proportional-Integral-Derivative (PID) controller) is widely employed because it is very understandable and high effective, besides, it has a simple conception. Even though the compensator is simple, it is quite sophisticated because it captures the history of the system (through integration) and anticipates the future behavior of the system (through differentiation). However, this integer order description can cause significant differences between mathematical model and the real system.

In addition, It is difficult to control system with nonlinearity using classical PID controllers. The known methodology is based on the linearization of the system at different operating points and controllers are designed for these points [15], which causes loosing some system's caracteristics. Nowadays, an important achievement is obtained, one of the possibilities to improve the PID controller is to use the fractional order controller with fractional derivation and integration. It becomes mostly sufficient for the nonlinear systems and can perform better than the integer order case.

In 1990 M. Axtell discussed the application of fractional calculus to the control systems. He introduced different integral operators by using Laplace transforms [16]. He recommended an extensive research of the fractional calculus in the control systems to identify its impact. Therefore, FOPID controllers are employed in the industrial domain and proved their effectiveness and robustness. Fractional controllers can also increase the stability of the system [17].

Robust path tracking of a mobile robot is presented in [18] as an example of application, where a complex nonlinear system with its speed characteristics was modeled and controlled using the fractional calculus associated with sliding mode to obtain the robust control of the torque. The torques generated for the rotors reach so higher values when sudden changes occur in the transitions of the desired position trajectory (30000 Nm).

Relatively, and without missing the system properties, the purpose of this work is to minimize the startup torque to make the rehabilitation session more attractive for children by reducing the pain caused at the beginning of the cycle. The Starting torque is the maximum torque that can be delivered to the mechanical load (exoskeleton) for its rotation. In the same time robots for rehabilitation tasks require a high degree of safety for the interaction with both the patients and for the operators. So minimal startup torque is considered as benefic to ensure this purpose. High values of torques can damage the system. Thus in this work that the startup torque will be considered as a performance index in the established comparison study. The computed torque control method has been employed as a solution to achieve this purpose in [19] for a two DOF upper limb rehabilitation robot.

Researchers tend to apply the artificial intelligence for these robots, in this work, it is used to develop the optimization method. In an other hand, and because of its additional parameters regarding an IOPID, tuning a fractional order controller is a challenging work [20]. In [21], a ASO algorithm is used to determine the proportional, integral and derivative orders of a fractional order PID used for the control of a DC motor Speed. This approach is considered simple and easy to implement.

Moreover, authors in [22] proposed an optimized FOPID controller using the ABC algorithm. It is a self-tuned regulator to minimize the given objective function in order to satisfy the inequality constraints of a brushless DC motor and to overcome the problems of nonlinearity but the robustness verification of the proposed FOPID controller under plant parameter variations is not proved. Authors in [23] attempted to explore and optimize a FOPID controller in order to obtain an optimal

automatic voltage regulator. The GBO method in this work is adopted to obtain the optimal values. In medicine applications, a Fractional Proportional Integral controller (FPI) tuned by Ant Colony Optimization (ACO) algorithm is synthesized to control a Prosthetic hands, simulations results prove that it enhances the positioning and reduces the system vibrations [24].

A FOPID has two additional tuning parameters than the conventional one [25], however in this paper there are nine parameters. This is due to the proposed approximation for the fractional calculus which demands four boundary frequencies for both the derivative and the integral terms. Thus, genetic algorithm (GA) is used in the process of the optimization. GA has the ability to deliver good solutions [26] [27] in this case. It is inspired from the theory of biological evolution proposed by Darwin and treats three main operators to the chromosomes (solutions) in each generation (iteration): selection, crossover (recombination), and mutation [28][29].

In this paper, we employ the GA for tuning variety of parameters created in selected search spaces of the FOPID controller for the lower limb exoskeleton (LLE). The motivation of GA is to minimize the trajectory error and the energy of the system for different rehabilitation gait training cycles. The proposed FOPID is implemented for a 2-DOF robot that stimulates the two high joints of the kid's lower limb (hip and knee). In fact, this controller solves also other problems such as the reduction of the control values and the system vibrations simultaneously.

The paper is structured as follows: Section 2 presents the mathematical model of the robot. Section 3 introduces the design of the two proposed controller and the optimization algorithm. Simulation results within Section 4 are divided into 2 parts. A comparison with an IOPID is established primarily and a discussion of the FOPID robustness versus parameters uncertainties is presented secondly. Finally, the last section is dedicated to the conclusion.

2. System Description and Dynamic Properties

As the robotic dynamic systems are nonlinear, highly coupled and time varying, its implementation requires a precise knowledge of the structure of the dynamic model [30]. The benefit of the dynamic model is to compute the torque and the force required in order to execute the typical work cycle and to give information for the design of the links, the joints, the drives, and the actuators as well as for the control scheme [19]. The design of the control strategy of robots generally includes the kinematic and the dynamic analysis. The dynamic model reflects the mathematical relationship between the motion of the robot and the driving torque. It can be expressed in the form of various characteristics like the differential equation or the transfer function compared theoretically or experimentally computation.

In this section, we suffice to present the obtained dynamic model of the lower limb exoskeleton dedicated to the gait rehabilitation for kids without presenting the calculus process (application of Lagrange formula). The used lower limb with 2-DOF is composed basically by the hip (angle α_1) and the knee (angle α_2) joints. It is a system with two arms, of l_1 and l_2 lengths and m_1 and m_2 masses. It includes both the kid limb and the exoskeleton [31] and is presented as follows

$$H(\alpha)\ddot{\alpha} + N(\dot{\alpha}, \alpha)\dot{\alpha} + G(\alpha) = u \tag{1}$$

where

- $\alpha = [\alpha_1 \alpha_2]^T \in R^2$ is the position vector,
- $\dot{\alpha} = [\dot{\alpha}_1 \dot{\alpha}_2]^T \in R^2$ is the speed vector,
- $\ddot{\alpha} = [\ddot{\alpha}_1 \ddot{\alpha}_2]^T \in R^2$ is the acceleration vector,

and

- $H(\alpha) \in R^{2\times2}$ is the inertia matrix, which is symmetric, uniformly bounded and positive definite,
- $N(\dot{\alpha}, \alpha) \in R^{2\times2}$ represents coriolis, centrifugal forces and torques,
- $G(\alpha) \in R^2$ denotes the gravity torque vector,
- $u \in R^2$ is the vector of actuator torques.

The system parameters are introduced as follows

- m_1, m_2, l_1, l_2 are the mass and the length of thigh and shank segments of the exoskeleton respectively,
- m_t, m_s represent the thigh and the shank masses of the human limb respectively,
- k_1, k_2 are the center position of the thigh and the shank segments masses respectively,
- I_1, I_2, I_s, I_t are the moments of inertia of thigh and shank of the exoskeleton and the human limb respectively,
- g is the gravity acceleration.

The parameters used for the synthesis and the simulation are approximated values a seven years old child.

3. Method

In the present case, the rehabilitation process satisfies an activity that deals with the walking cycle of a healthy child aged between 3 and 12 years (α_d). Initially, the error signal $e(t)$ resulting from the difference between the desired and the real trajectories is used to evaluate the objective function of the genetic algorithm. Parameters obtained from the optimization are the tuned arguments of the controller. Then, the torque produced by the FOPID controller is feeded to the robot to obtain the following equation deduced from (1) as

$$\ddot{\alpha}(t) = H^{-1}(\alpha)\left(u(t) - N(\dot{\alpha}, \alpha)\dot{\alpha}(t) - G(\alpha)\right) \tag{2}$$

The position $\alpha(t)$ is obtained by integrating twice times (2). This section deals with three parts: the description of the proposed fractional and integer order controller and the parameters optimization method.

3.1. FOPID Controller

The proposed feed-back loop control system is presented in Fig. 1. In the last years, researchers have increased the attention to apply the fractional calculus in the control systems engineering. This field includes the application of fractional-order differentiation/integration operators in the modeling of real-world processes and for proposing effective control laws. The fractional order PID (FOPID) controller is the expansion of the conventional PID controller based on fractional calculus. It has been very popular in industries for the control applications to enhance the performance of the plants having nonlinear characteristics.

Accordingly, the FOPID computes the torque u through the following differential (3) as

$$u(t) = \left(K_p e(t) + K_i I^{\lambda} e(t) + K_d D^{\mu} e(t)\right) \tag{3}$$

with

- $e(t) = \alpha_d(t) - \alpha(t)$ is the differentiation between the desired and the real trajectories noted the error.
- λ and $\mu \in]0, 1[$ are the fractional orders of the integrator and the derivator respectively.
- K_p, K_i and K_d are the proportional, the integral and the derivative gains of the FOPID controller, respectively.

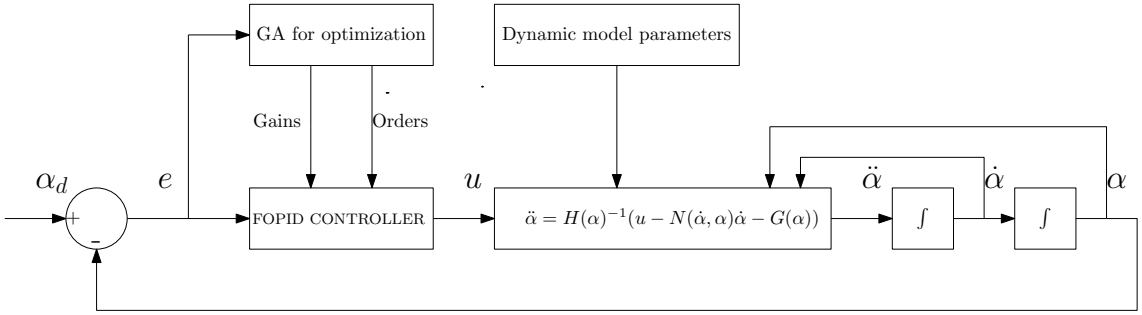

Fig. 1. Closed loop control schema of the system

Indeed, there is a large number of methods for the design of integer order controllers. However, in the case of fractional order controllers, only few methods are being worked out. Oustaloup approximation [32] is widely used in the design of such controllers. It is a recursive distribution of zeros and poles where the derivative operator is estimated with (4) as

$$D^{\mu} = \prod_{j=-N}^{N} \frac{1 + \frac{s}{\omega'_{Dj}}}{1 + \frac{s}{\omega_{Dj}}} \tag{4}$$

where $(-\omega'_{Dj})$ and $(-\omega_{Dj})$ are the zero and the pole of rank j respectively, recursively distributed in the frequency range $[\omega_{Dl}, \omega_{Dh}]$, and defined in (5) and (6).

$$\omega'_{Dj} = \omega_{Dl}\left(\frac{\omega_{Dh}}{\omega_{Dl}}\right)^{\frac{j+N+0.5(1-\mu)}{2N+1}} \tag{5}$$

$$\omega_{Dj} = \omega_{Dl}\left(\frac{\omega_{Dh}}{\omega_{Dl}}\right)^{\frac{j+N+0.5(1+\mu)}{2N+1}} \tag{6}$$

where $2N + 1$ is the number of cells, in this case we choose $N = 3$ which is equivalent to 7 blocks of transfer functions. And for a good approximation of the fractional-order, two or three decades at least should be considered between $[\omega_{Dl}, \omega_{Dh}]$ [33].

The synthesis of the the integral operator of order λ is achieved with analogy to equation (4) respecting the zeros $(-\omega'_{Ij})$ and the poles $(-\omega_{Ij})$ definition which are regularly distributed in the frequency range $[\omega_{Il}, \omega_{Ih}]$. Finally the continuous transfer function of a FOPID is obtained through Laplace transform, and given by (7) as

$$u(s) = \left(K_p + K_i\left(\frac{\omega_I}{s}\right)^{\lambda} + K_d\left(\frac{s}{\omega_D}\right)^{\mu}\right)e(s) \tag{7}$$

with

$$\omega_I \epsilon [\omega_{Il}, \omega_{Ih}] \tag{8}$$

and

$$\omega_D \epsilon [\omega_{Dl}, \omega_{Dh}] \tag{9}$$

For more clarity, Fig. 2 presents the block of the approximated FOPID controller by Oustaloup method [34].

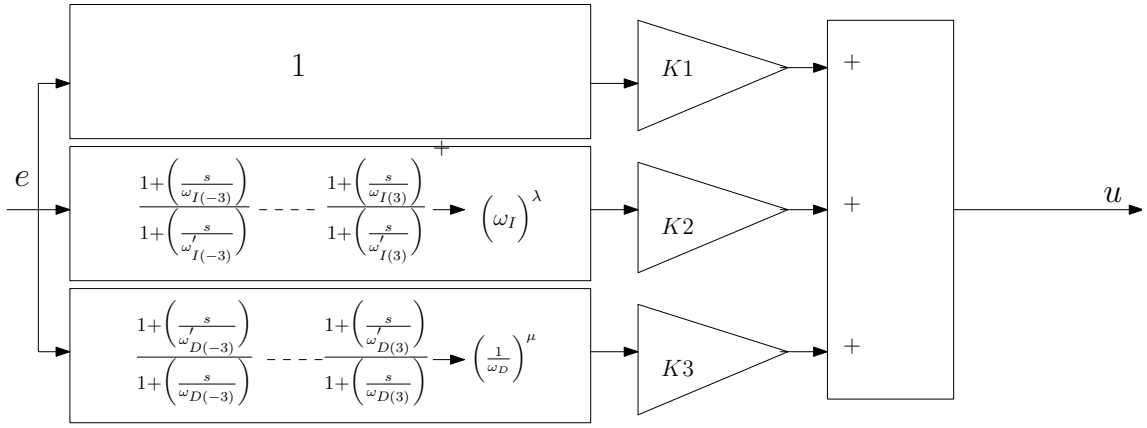

Fig. 2. FOPID controller

3.2. IOPID Controller

A numerical comparison with an IOPID is introduced to evaluate the performance of the FOPID. The IOPID is described by (10) as

$$u(s) = \left(K_p + K_i \left(\frac{\omega_I}{s} \right) + K_d \left(\frac{s}{\omega_D} \right) \right) e(s) \tag{10}$$

It admits this model as the FOPID controller with λ=1 and μ=1 saving the same elements of gains and frequencies. using this form of the IOPID is for the purpose of dissipating torque in the begining of the startup gait cycle. The parameters of the $PI^{\lambda}D^{\mu}1$, the $PI^{\lambda}D^{\mu}2$, the IOPID 1 and the IOPID 2 for the control of the joint 1 and the joint 2 are optimized by means of a genetic algorithm which generates the following solutions:

- The six gains K_p, K_i, K_d and $K_p^{'}, K_i^{'}$ and $K_d^{'}$ for both controllers
- The orders λ and μ for the FOPID controller
- The frequencies $\omega_{Il}, \omega_{Ih}, \omega_I, \omega_{Dl}, \omega_{Dh}$ and ω_D for both controllers

3.3. Genetic Algorithm For Optimization

The tuning of the FOPID is one of the main concerns in the design of the controller. Researchers have used different methods of tuning, such as genetic algorithm GA. It was developed by Holland in 1975 and considered as a tool for searching solutions to optimization problems with complex characteristics and large solution search spaces [35]. It can be classified within the numerical methods for parameters tuning, based on the process of the natural selection that has a biological evolution. Therefore, this approach applies a direct random search technique to find the optimal solution in a complex multi-dimensional space.

GA does not involve much background about the complexity of the system (it treats in our case, only error and energy), Fig. 3 summarizes the main steps of the problem's resolution. The reasons of the use of GA are numerous: (i) multiple parameters to tune (orders gains and frequencies), (ii) different searching spaces to consider ($(B_{low}$ and $B_{high})$ and (iii) also because of the selected multi-objective functions.

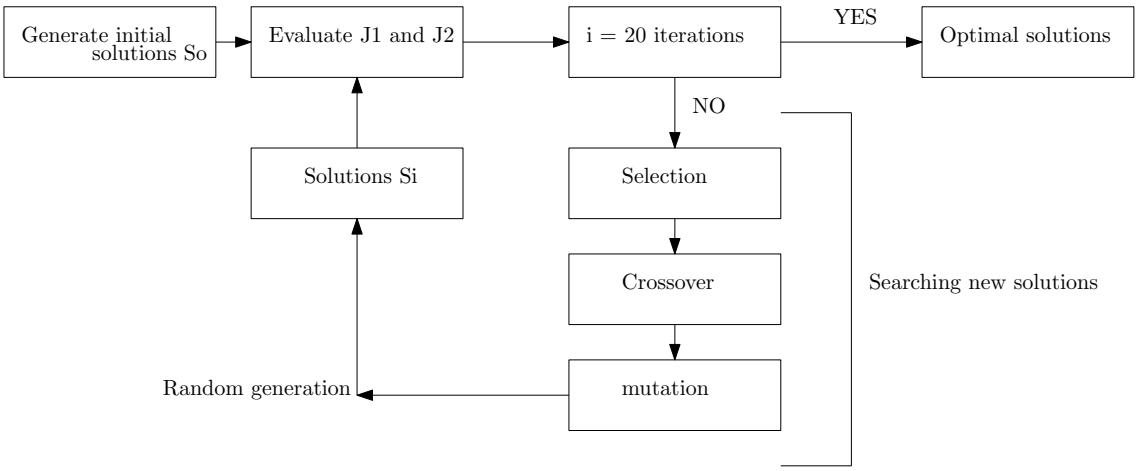

Fig. 3. Genetic algorithm process

In this scenario, GA proves to be an efficient tool to provide usable near-optimal solutions in a short amount of time (rapidly) in comparison with the traditional calculus based methods. The undertaken design control problem is to find the optimal tuned parameters of the given FOPID that ensure a certain objective function. The objective function suggested to force the robot to behave similar to the predefined trajectory. Each GA solution has to minimize the following objective functions which are defined as (11) and (12) as

$$J1 = IAE1 + IAE2 \tag{11}$$

and

$$J2 = IAU1 + IAU2 \tag{12}$$

where IAE1 and IAE2 are the integral of absolute errors and IAU1 and IAU2 are the used energies of joints 1 and 2 respectively which are detailed in next section.

These objective functions evaluate the FOPID parameters and generate a high quality solutions. Initially, random values of solutions are chosen basically from our previous works to start the optimization process. Then each solution is evaluated with the fitness calculation. Three phenomenons are performed subsequently in this level: reproduction, crossover and mutation to produce the new generation of solutions. Hence, the new chromosomes ($K_1, K_2, K_3, K_1^{'}, K_2^{'}, K_3^{'}, \lambda, \mu, \omega_{Il}, \omega_{Ih}, \omega_D \ \omega_{Dl}, \omega_{Dh}\, \omega_I$) are tested and their fitness is investigated again.

The final solution is obtained after the selected number of iterations and the result values are chosen to simulate the controlled system and are tabulated as follows in Table 1 and Table 2. The tuned high frequencies ω_{Ih} and ω_{Dh} respectively of the integral and the derivative terms are automatically optimized because they are calculated via the following (13) and (14) as

$$\omega_{Ih} = 10^3 \omega_{Il} \tag{13}$$

and

$$\omega_{Dh} = 10^3 \omega_{Dl} \tag{14}$$

The flowchart of genetic algorithm process is detailed in Fig. 4 which presents the main simulation steps of the obtention optimal parameters used for the approximation of fractional calculus.

Table 1. Optimized parameters values of the FOPID controller

Tuned parameter	designation	optimal value
K_p	the proportional gain of FOPID 1	200.168
K_i	The integral gain of FOPID 1	250.059
K_d	The derivative gain of FOPID 1	200.059
$K_p^{'}$	The proportional gain of FOPID 2	100.168
$K_i^{'}$	The integral gain of FOPID 2	100.059
$K_d^{'}$	The derivative gain of FOPID 2	70.059
λ	The integral order	0.700
μ	The derivative order	0.700
ω_{Il}	The low frequency of the integral part	0.826
ω_I	The integral frequency gain	1.102
ω_{Dl}	The low frequency of the derivative part	3.825
ω_D	The derivative frequency gain	5.102

Table 2. Optimized parameters values of the IOPID controller

Tuned parameter	designation	optimal value
K_p	The proportional gain of IOPID 1	308.804
K_i	The integral gain of IOPID 1	143.243
K_d	The derivative gain of IOPID 1	143.243
$K_p^{'}$	The proportional gain of IOPID 2	238.853
$K_i^{'}$	The integral gain of IOPID 2	143.243
$K_d^{'}$	The derivative gain of IOPID 2	72.121
λ	The integral order	1.000
μ	The derivative order	1.000
ω_{Il}	The low frequency of the integral part	0.143
ω_I	The integral frequency gain	1.014
ω_{Dl}	The low frequency of the derivative part	10.143
ω_D	The derivative frequency gain	14.143

4. Comparison and Simulation Results

The comparison is based on four performance indexes during five cycles:

- The IAE (Integral of Absolute Error) computed by (15):

$$IAE = \int_0^t e(t)dt \tag{15}$$

- The Startup Torque (ST): is the required torque to start rotating for the applied load $u(t = 0)$
- The ISE (Integral square error) computed by (16):

$$ISE = \int_0^t e^2(t)dt \tag{16}$$

- The IAU (the Integral of Absolute Control Action (torque)) computed as (17):

$$IAU = \int_0^t u(t)dt \tag{17}$$

Effectively, these comparison studies include two cases, the nominal case and with uncertainties case.

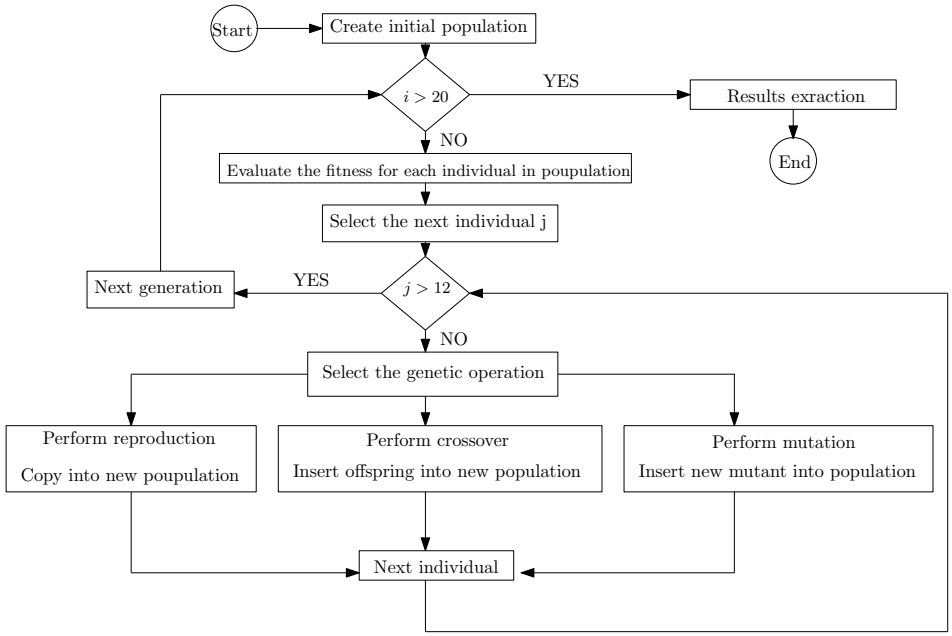

Fig. 4. the flow chart of the genetic algorithm process

4.1. Case 1: Nominal Case

In this case, the results are obtained by applying the optimized FOPID to control the 2 DOF exoskeleton dedicated for children with cerebral palsy where the parameters of both robot and patient are used with their mean values. As it is depicted in Fig. 5 where the joint 1 of the robot (the hip) follows the desired trajectory with a non-considerable error, the IAE1 value equals 0.040. The same curves are presented in Fig. 6 for the joint 2 (the knee) where the IAE2 equals 0.067.

In the second configuration, where the IOPID is used to command the system, same figures show that the real trajectories attend the same predefined trajectories (of a healthy child) but with an IAE equals to 0.065 and 0.0.069 for the joint 1 and the joint 2 respectively. Based on the same figures, it is well obvious also, that the robot controlled with the fractional PID achieve the steady state before a notable time and with less overshoot than the integer PID and that is also demonstrated with the ISE obtained values.

The flexibility of the fractional calculus contributes to these results and proves the superiority of the FOPID vs the IOPID. Startup torques are also compared, Fig. 7 and Fig. 8 reveal the torques of the joints 1 and 2 using FOPID and IOPID co achieves. Torques of the joints 1 and 2 while using the IOPID controller are presented also in the same figures. Based on these curves, the startup torque of the joint 1 is of 47.2 Nm and 49.9 Nm applying respectively the FOPID and the IOPID in the control process which means an amelioration of 5%.

For the second joint, the startup torque with the FOPID is 35% lower than its in IOPID case (74.3 Nm VS 114.2 Nm). The same system was controlled in [36] with the L1 adaptive approach, but the startup torque values were so high. In fact for the joint 1, it equals 600 Nm and 1500 Nm for the joint 2. This proves the efficiency of the proposed controller.

The energy IAU generated with the fractional controller reached 16.36 for the joint 1 and 11.66 for the joint 2 and it is less than the IAU produced with the integer order controller which achieved 29.04 and 20.05 for the joint 1 and 2 respectively. Because the torque is directly proportional to the square of the supply voltage, the system with fractional controller is more preferment in term of cost in comparison with integer controller.

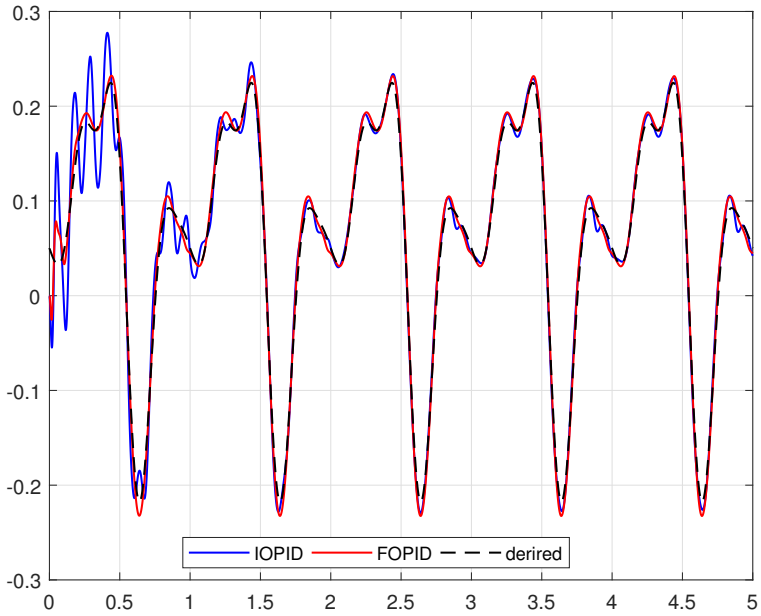

Fig. 5. Controlled hip joint (rad) during 5 gait cycles (X-axis)

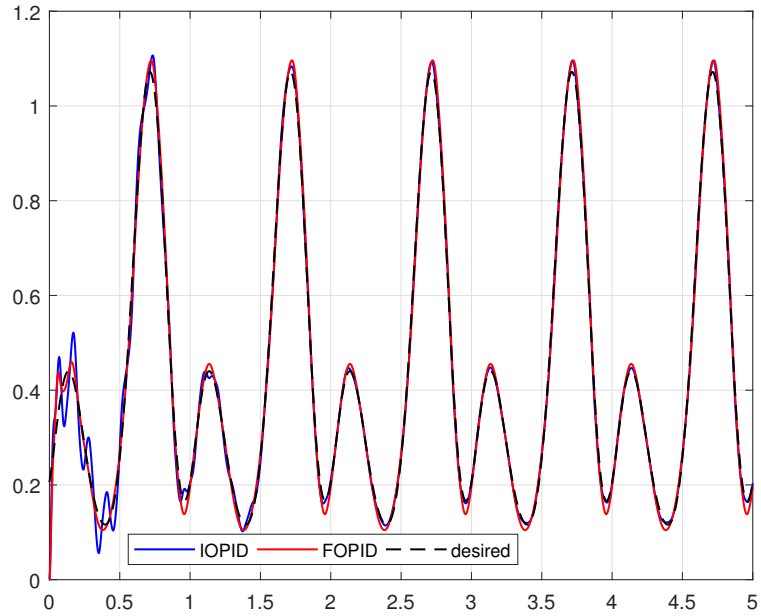

Fig. 6. Controlled knee joint (rad) during 5 gait cycles (X-axis)

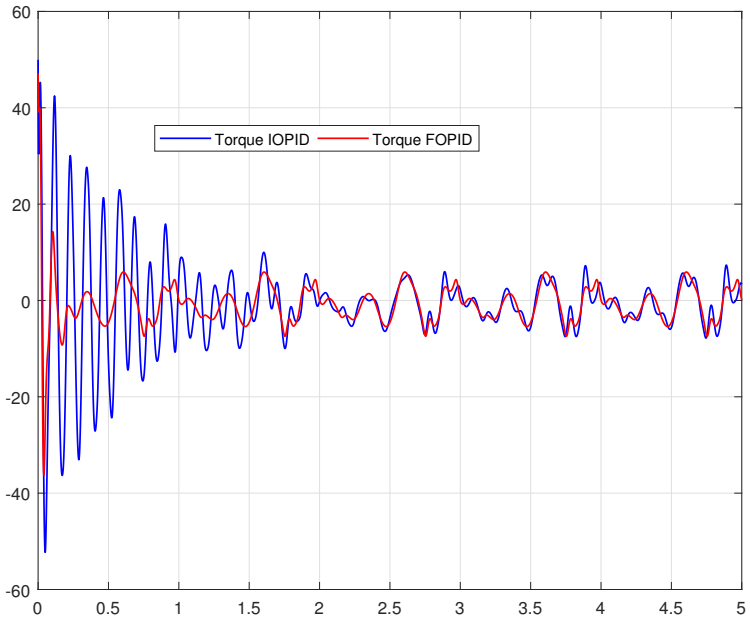

Fig. 7. Produced torques 1 using the both controllers

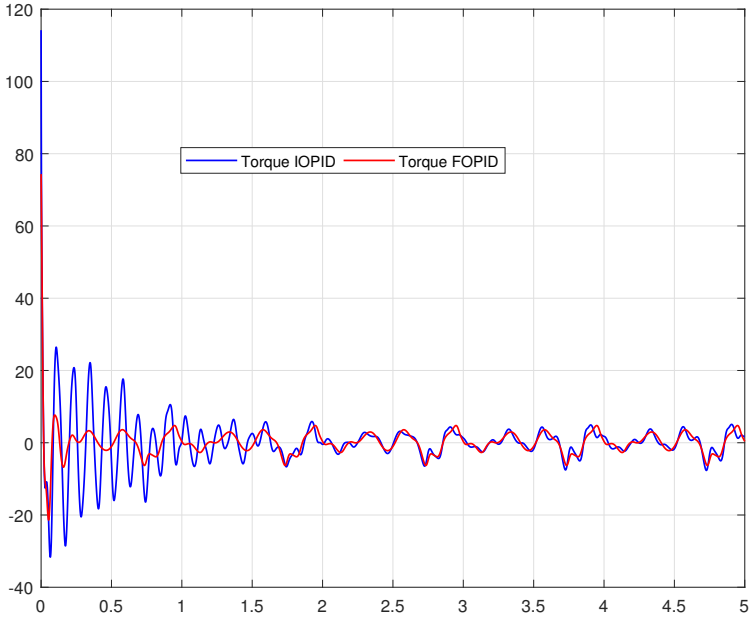

Fig. 8. Produced torques 2 using the both controller

Velocities of joints 1 and 2 of the both used controllers FOPID and IOPID controllers are respectively given in Fig. 9 and Fig. 10. To summarize, IAE, IAU, ISE and startup torque collected values are tabulated in Table 3. Table 4 shows the percentage of improvement of the performance indexes, and as it is revealed, the FOPID is outperforming the IOPID for both joints 1 and 2.

The difference between the two controllers essentially seems on the orders of the integer and the derivative terms. So to prove the efficiency of the proposed genetic algorithm with the traditional technique (which study the objective function value instead of random parameter value), we present the two diagrams illustrating the variation of the objective functions vs orders. The J1 objective function is presented in Fig. 11 where the optimal value is obtained around μ=0.7. Corresponding, Fig. 12 shows that the optimal value of J2 objective function manifests around λ =0.7 too. These values are achieved rapidly by employing GA algorithm process.

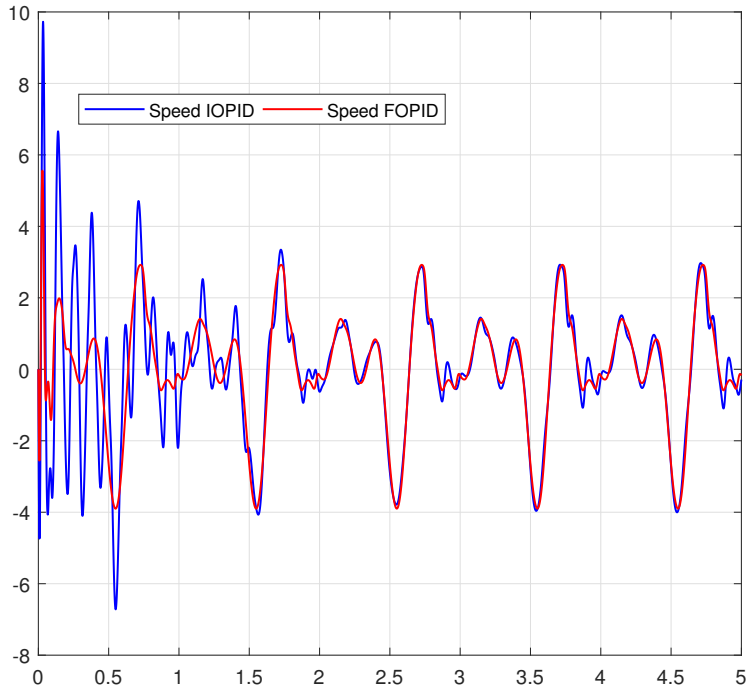

Fig. 9. Speeds 1 using the two controllers

Table 3. Performance values for both controllers

Performance	IOPID	FOPID
$IAE1$	0.065	0.040
$IAE2$	0.069	0.067
$ST1(Nm)$	49.96	47.2
$ST2(Nm)$	114.2	74.35
$ISE1$	0.0022	0.0005
$ISE2$	0.002	0.001
$IAU1$	29.04	16.36
$IAU2$	20.05	11.66

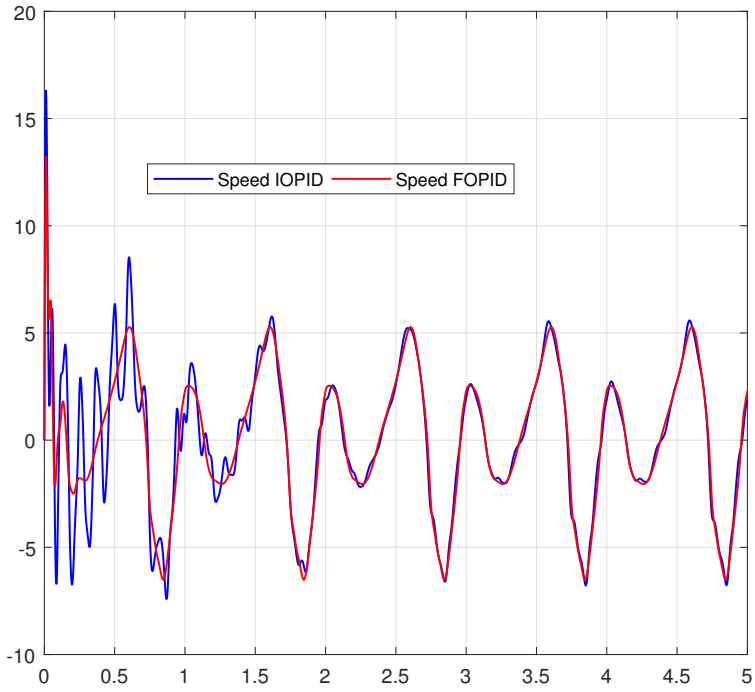

Fig. 10. Speeds 2 using the two controllers

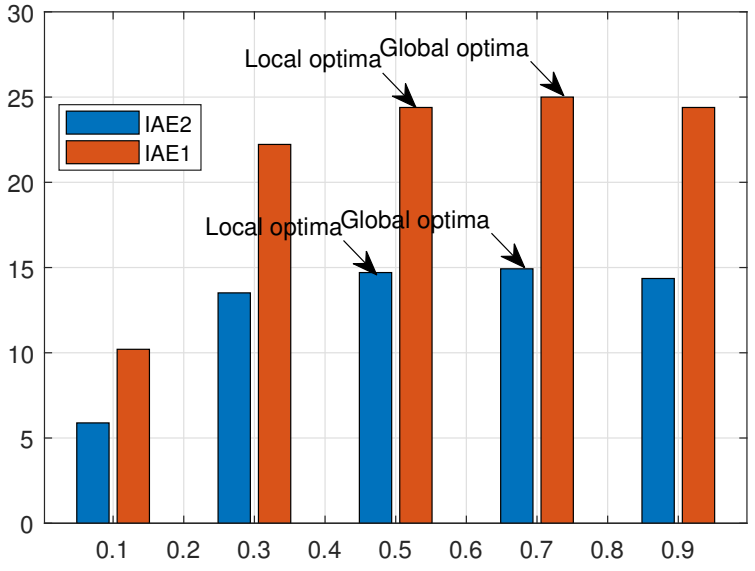

Fig. 11. Tracking trial and error ($J1^{-1}$ vs μ)

Table 4. Improvement in % of IAE, ST, ISE and IAU with FOPID controller

FOPID *vs* IOPID							
IAE1	IAE2	ST1	ST2	ISE1	ISE2	IAU1	IAU2
38.46%	2.89%	5.52%	34.89%	77%	50%	43.66%	41.84%

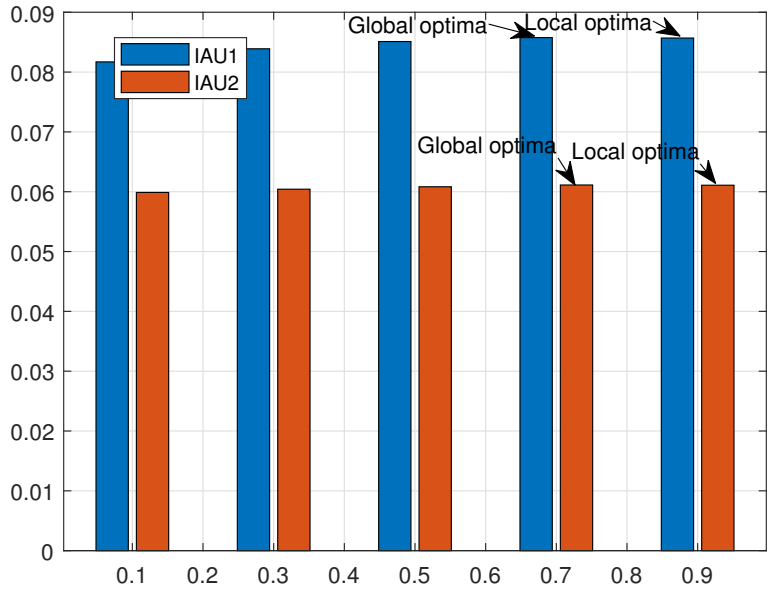

Fig. 12. Energy trial and error ($J2^{-1}$ vs λ)

4.2. Case 2: Parameter Uncertainties

The efficiency of the proposed controller is also evaluated in the case of parameter uncertainties. This variation includes the system's parameters (the thigh and the shank masses of the kid limb: mt, ms). Two cases are retained: 5% and 10% of uncertainties variation. The work will focus on the efficiency of the FOPID controller against the parametric variation. Table 5 presents the evolution of the IAE1, IAE2, ISE1 and ISE2 against the shank mass variation. As it is shown, the same values are obtained via numerical simulation. From 1% to 10 % of this variation, there is a leger difference that doesn't exceed 6%. Moreover, Table 6 shows the same evolution versus the thigh mass variation. The numerical simulation until 10% of variation clearly indicates that the collected values of IAE1 and IAE2, ISE1 and ISE2 are constant which proves the robustness of the controlled system.

Table 5. Performance indexes in the case of the shank parameter uncertainties

Performance index	**5% variation**	**10% variation**
IAE1	0.041	0.042
IAE2	0.070	0.072
ISE1	0.0005	0.0005
ISE2	0.001	0.002

The FOPID is insensitive to the parameter variation, and offers more flexibility in the control process and thus is demonstrated also in Fig. 13 and Fig. 14. The FOPID proves its performances in controlling the studied robotic system for gait rehabilitation. In fact, it permits to reduce the robot tracking error, ameliorate the startup torque and limit the generated energy. Besides, the FOPID

proves its efficiency also in the case of parameter uncertainties to control perfectly the system.

Table 6. Performance indexes in the case of the thigh parameter uncertainties

Performance index	5% variation	10% variation
IAE1	0.040	0.040
IAE2	0.067	0.067
ISE1	0.0005	0.0005
ISE2	0.001	0.001

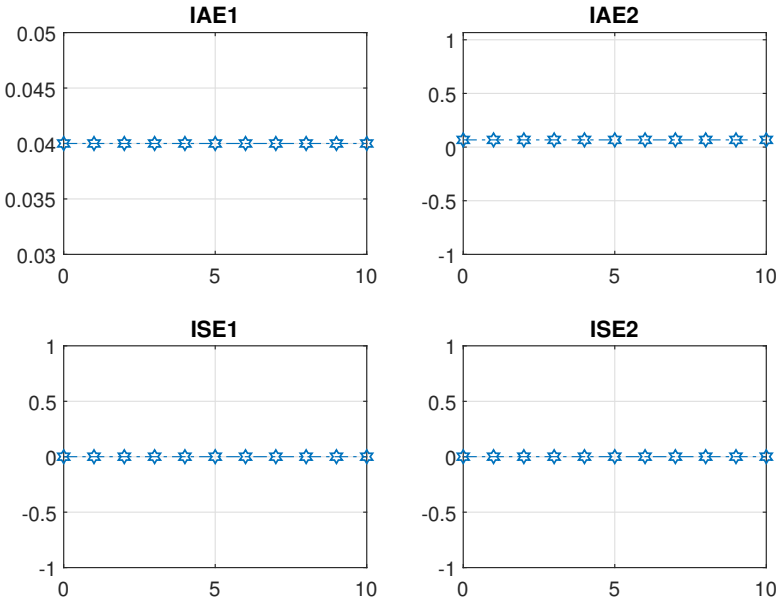

Fig. 13. Error evolution against thigh mass variation (mt in % (X-axis))

5. Conclusion

The current work deals with a control solution dedicated to a lower limb exoskeleton used for the gait rehabilitation of the kids suffering from Cerebral Palsy. The algorithm evolves a population of individuals (solutions) with genetic operators that seek to maximize the performance of the system with minimizing the error in tracking the desired trajectory as well as the energy and torques that make the actions of a human comfortable enough. Thus a FOPID controller is proposed and optimized using GA process. Through simulation results, a comparative study with an IOPID highlighted the efficacy of the FOPID. In fact, the FOPID controller shows better performance indexes in term of tracking error, startup torque and used energy for both joints (hip and knee). Robustness is also proved by simulating the system with some parameter uncertainties. It includes two variations in parameters (shank and thigh masses). The FOPID robustness is verified via IAE and ISE calculation and the well tracking of the desired trajectory is proved. As a future work, we tend to achieve the stability study of the system. Also we plan to finish measuring EMG walking to use it in fractional calculus to control the prototype of the robot.

Author Contribution: All authors contributed equally to this paper. All authors read and approved the final paper.
Funding: This work is supported by the university of sfax, Tunisia and more data are available from

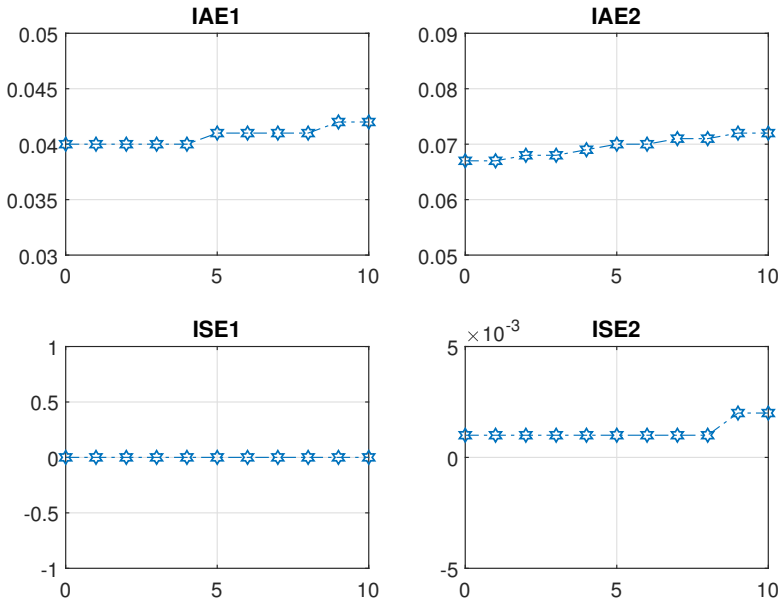

Fig. 14. Error evolution against shank mass variation (ms in % (X-axis))

the corresponding author.

Acknowledgment: The authors would like to acknowledge the Control and Energy Management Laboratory, University of Sfax and the Ministry of Higher Education, Tunisia for their supports to the success of this work.

Conflicts of Interest: The authors declare that they have no conflicts of interest.

References

[1] V. Cimolin, C. Germiniasi, M. Galli, C. Condoluci, E. Beretta, L. Piccinini, "Robot-Assisted upper limb training for hemiplegic children with cerebral palsy," *Journal of Developmental and Physical Disabilities*, vol. 31, no. 1, pp. 89-101, 2019, https://doi.org/10.1007/s10882-018-9632-y.

[2] J. A. Buitrago, A. M. Bolanos, E. Caicedo Bravo, "A motor learning therapeutic intervention for a child with cerebral palsy through a social assistive robot," *Disability and Rehabilitation: Assistive Technology*, vol. 15, no. 3, pp. 357-362, 2020, https://doi.org/10.1080/17483107.2019.1578999.

[3] A. A. Lins, J. M. de Oliveira, J. J. Rodrigues, V. H. C. de Albuquerque, "Robot-assisted therapy for rehabilitation of children with cerebral palsy-a complementary and alternative approach," *Computers in Human Behavior*, vol. 100, pp. 152-167, 2019 https://doi.org/10.1016/j.chb.2018.05.012.

[4] R. M. Andrade, S. Sapienza, P. Bonato, "Development of a transparent operation mode for a lower-limb exoskeleton designed for children with cerebral palsy," *IEEE 16th International Conference on Rehabilitation Robotics (ICORR)*, pp. 512-517, 2019, https://doi.org/10.1109/ICORR.2019.8779432.

[5] G. Zeilig, H. Weingarden, M. Zwecker, I. Dudkiewicz, A. Bloch, A. Esquenazi, "Safety and tolerance of the ReWalk exoskeleton suit for ambulation by people with complete spinal cord injury: A pilot study," *The journal of spinal cord medicine*, vol. 35, no. 2, pp. 96-101, 2012, https://doi.org/10.1179/2045772312Y.0000000003.

[6] A. Tsukahara, R. Kawanishi, Y. Hasegawa, Y. Sankai, "Sit-to-stand and stand-to-sit transfer support for complete paraplegic patients with robot suit HAL," *Advanced robotics*, vol. 24, no. 11, pp. 1615-1638, 2010, https://doi.org/10.1163/016918610X512622.

[7] K. A. Strausser and H. Kazerooni, "The development and testing of a human machine interface for a mobile medical exoskeleton," *IEEE/RSJ International Conference on Intelligent Robots and Systems*, pp. 4911-4916, 2011, https://doi.org/10.1109/IROS.2011.6095025.

[8] M. Bortole, A. Venkatakrishnan, F. Zhu, J. C. Moreno, G. E. Francisco, J. L. Pons, J. L. Contreras-Vidal, "The H2 robotic exoskeleton for gait rehabilitation after stroke: early findings from a clinical study," *Journal of neuroengineering and rehabilitation*, vol. 12, no. 1, pp. 1-14, 2015, https://doi.org/10.1186/s12984-015-0048-y.

[9] Y. Sun, Y. Tang, J. Zheng, D. Dong, X. Chen, L. Bai, "From sensing to control of lower limb exoskeleton: a systematic review," *Annual Reviews in Control*, 2022, https://doi.org/10.1016/j.arcontrol.2022.04.003.

[10] Z. Shen, J. Zhou, J. Gao, R. Song, "Fuzzy logic based PID control of a 3 DOF lower limb rehabilitation robot," *IEEE 8th Annual International Conference on CYBER Technology in Automation, Control, and Intelligent Systems (CYBER)*, pp. 818-821, 2018, https://doi.org/10.1109/CYBER.2018.8688089.

[11] Y. Yang, D. Huang, X. Dong, "Enhanced neural network control of lower limb rehabilitation exoskeleton by add-on repetitive learning," *Neurocomputing*, vol. 323, pp. 256-264, 2019, https://doi.org/10.1016/j.neucom.2018.09.085.

[12] S. K. Hasan and A. K. Dhingra, "An adaptive controller for human lower extremity exoskeleton robot," *Microsystem Technologies*, pp. 1-18, 2021, https://doi.org/10.1007/s00542-020-05207-8.

[13] A. Riani, T. Madani, A. Benallegue, K. Djouani, "Adaptive integral terminal sliding mode control for upper-limb rehabilitation exoskeleton," *Control Engineering Practice*, vol. 75, pp. 108-117, 2018, https://doi.org/10.1016/j.conengprac.2018.02.013.

[14] Munadi, M. S. Nasir, M. Ariyanto, N. Iskandar, J. D. Setiawan, "Design and simulation of PID controller for lower limb exoskeleton robot," *AIP Conference Proceedings*, vol. 1983, p. 060008, 2018, https://doi.org/10.1063/1.5046300.

[15] E. H. Dulf, "Simplified fractional order controller design algorithm," *Mathematics*, vol. 7, no. 12, p. 1166, 2019, https://doi.org/10.3390/math7121166.

[16] P. Shah and S. Agashe, "Review of fractional PID controller," *Mechatronics*, vol. 38, pp. 29-41, 2016, https://doi.org/10.1016/j.mechatronics.2016.06.005.

[17] H. Hamidian and M. T. Beheshti, "A robust fractional-order PID controller design based on active queue management for TCP network," *International Journal of Systems Science*, vol. 49, no. 1, pp. 211-216, 2018, https://doi.org/10.1080/00207721.2017.1397801.

[18] H. H. Ammar and A. T. Azar, "Robust path tracking of mobile robot using fractional order PID controller," *International Conference on Advanced Machine Learning Technologies and Applications*, pp. 370-381, 2019, https://doi.org/10.1007/978-3-030-14118-9_37.

[19] A. N. Sharkawy and P. Koustoumpardis, "Dynamics and computed-torque control of a 2-DOF manipulator: Mathematical analysis," *International Journal of Advanced Science and Technology*, vol. 28, no. 12, pp. 201-212, 2019, https://hal.archives-ouvertes.fr/hal-03598924.

[20] M. Z. Othman and E. A. Al-Sabawi, "Design of Fractional Order PID Controller Based on Genetic Algorithms," *Al-Rafadain Engineering Journal*, vol. 20, no. 4, 2012, http://dx.doi.org/10.33899/rengj.2012.54151.

[21] B. Hekimoglu, "Optimal tuning of fractional order PID controller for DC motor speed control via chaotic atom search optimization algorithm," *IEEE Access*, vol. 7, pp. 38100-38114, 2019, https://doi.org/10.1109/ACCESS.2019.2905961.

[22] K. Vanchinathan and N. Selvaganesan, "Adaptive fractional order PID controller tuning for brushless DC motor using artificial bee colony algorithm," *Results in Control and Optimization*, vol. 4, p. 100032, 2021, https://doi.org/10.1016/j.rico.2021.100032.

[23] S. M. A. Altbawi, A. S. B. Mokhtar, T. A. Jumani, I. Khan, N. N. Hamadneh, and A. Khan, "Optimal design of Fractional order PID controller based Automatic voltage regulator system using gradient-based optimization algorithm," *Journal of King Saud University-Engineering Sciences*, 2021, https://doi.org/10.1016/j.jksues.2021.07.009.

[24] R. Jallouli-Khlif, B. Maalej, P. Melchior, and N. Derbel, "Control of Prosthetic Hand Based on Input Shaping Combined to Fractional PI Controller," *9th International Conference on Systems and Control (ICSC)*, pp. 449-454, 2021, https://doi.org/10.1109/ICSC50472.2021.9666537.

[25] Y. Zhang and J. Li, "Fractional-order PID controller tuning based on genetic algorithm," *International Conference on Business Management and Electronic Information*, pp. 764-767, 2011, https://doi.org/10.1109/ICBMEI.2011.5920371.

[26] S. Mirjalili, J. S. Dong, A. S. Sadiq, and H. Faris, "Genetic algorithm: Theory, literature review, and application in image reconstruction," *Nature-inspired optimizers*, pp. 69-85, 2020, https://doi.org/10.1007/978-3-030-12127-3_5.

[27] D. Doval, S. Mancoridis, B. S. Mitchell, "Automatic clustering of software systems using a genetic algorithm," *Proceedings Ninth International Workshop Software Technology and Engineering Practice*, pp. 73-81, 1999, https://doi.org/10.1109/STEP.1999.798481.

[28] M. K. Amjad, S. I. Butt, R. Kousar, R. Ahmad, M. H. Agha, Z. Faping, N. Anjum, and U. Asgher, "Recent research trends in genetic algorithm based flexible job shop scheduling problems," *Mathematical Problems in Engineering*, 2018, https://doi.org/10.1155/2018/9270802.

[29] L. B. Booker, D. E. Goldberg, J. H. Holland, "Classifier systems and genetic algorithms," *Artificial intelligence*, vol. 40, no. 1-3, pp. 235-282, 1989, https://doi.org/10.1016/0004-3702(89)90050-7.

[30] H. F. Ho, Y. K. Wong, A. B. Rad, "Robust fuzzy tracking control for robotic manipulators," *Simulation Modelling Practice and Theory*, vol. 15, no. 7, pp. 801-816, 2007, https://doi.org/10.1016/j.simpat.2007.04.008.

[31] M. Ghezal, M. Guiatni, I. Boussioud, and C. S. Renane, "Design and Robust Control of a 2 DOFs Lower Limb Exoskeleton," *International Conference on Communications and Electrical Engineering (ICCEE)*, pp. 1-6, 2018, https://doi.org/10.1109/CCEE.2018.8634540.

[32] A. Oustaloup and B. Mathieu, *La commande CRONE: du scalaire au multivariable*, Hermes Editions: Paris, 1999, https://books.google.co.id/books?id=ccBbAAAACAAJ.

[33] B. Maalej, R. J. Khlif, C. Mhiri, M. H. Elleuch, N. Derbel, "Adaptive fractional control optimized by genetic algorithms with application to polyarticulated robotic systems," *Mathematical Problems in Engineering*, 2021, https://doi.org/10.1155/2021/5579541.

[34] I. Petras, "Fractional Derivatives, Fractional Integrals, and Fractional Differential Equations in Matlab," *Engineering Education and Research Using MATLAB*, 2011, https://doi.org/10.5772/19412.

[35] R. Al-Aomar, "Incorporating robustness into genetic algorithm search of stochastic simulation outputs," *Simulation modelling practice and theory*, vol. 14, no. 3, pp. 201-223, 2006, https://doi.org/10.1016/j.simpat.2005.05.001.

[36] B. Maalej, A. Chemori, and N. Derbel, "Intelligent Tuning of Augmented L_1 Adaptive Control for Cerebral Palsy Kids Rehabilitation," *16th International Multi-Conference on Systems, Signals Devices (SSD)*, pp. 231-237, 2019, https://doi.org/10.1109/SSD.2019.8893237.